ACADEMIC PRESS

Available online at www.sciencedirect.com

SCIENCE DIRECT®

Journal of Magnetic Resonance 163 (2003) 332–339

JMR Journal of Magnetic Resonance

www.elsevier.com/locate/jmr

Low-power XiX decoupling in MAS NMR experiments

Matthias Ernst,[a,*] Ago Samoson,[b] and Beat H. Meier[a]

[a] *Physical Chemistry, ETH-Zurich, CH-8093 Zurich, Switzerland*
[b] *National Institute of Chemical Physics and Biophysics, Akadeemia Tee 23, Tallinn 12618, Estonia*

Received 28 February 2003; revised 24 April 2003

Abstract

Low-power XiX proton decoupling under fast magic-angle spinning is introduced. The method is applicable if the MAS frequency exceeds the proton–proton interactions. For rigid organic solids this is the case for MAS frequencies above approximately 40 kHz. It is shown that the quality of the decoupling as well as the sensitivity to frequency offsets can be improved compared to low-power continuous-wave decoupling. The decoupling efficiency is somewhat reduced compared to optimized high-power decoupling: in a peptide sample investigated at an MAS frequency of 50 kHz a loss of about 10% in signal intensity for CH_3 and CH groups, and of about 40% for CH_2 groups was observed. Taking into consideration, that the rf amplitude in the low-power XiX was about 15 times lower than in high-power XiX decoupling, such a reduction in line intensity is sometimes tolerable.

1. Introduction

Efficient heteronuclear spin decoupling is a key requirement for high-resolution solid-state NMR spectroscopy. In magic-angle spinning experiments of solid samples, the homogeneous line broadening caused by incomplete proton decoupling is often an important contribution to the total linewidth of ^{13}C and ^{15}N resonances. Other possible contributions to the linewidth include the distribution of isotropic chemical shifts due to structural inhomogeneities of the sample and unresolved homonuclear *J*-couplings. With the invention of two-pulse phase-modulated decoupling (TPPM) [1] and related pulse schemes [2–6] considerable progress has been made in reducing the residual heteronuclear couplings. Phase-inversion decoupling under MAS [7] has been shown to be particularly efficient at higher spinning frequencies, i.e., above 25 kHz. The X-inverse-X decoupling scheme (XiX) [8] consists of two pulses of equal length τ_p which are phase shifted by 180 °. The optimum pulse length was found to be close to $\tau_p = 2.85\tau_r$, where τ_r is the inverse of the MAS frequency.

All the decoupling schemes mentioned so far give best results at the highest possible rf-field strength assuming that rotary-resonance recoupling conditions are avoided [9,10]. They have all been developed for the "high-power decoupling" regime where the nutation frequency of the rf-field, ω_1, is significantly higher than the heteronuclear and homonuclear couplings as well as the MAS frequency, ω_r. Typical rf-field amplitudes are 50–250 kHz depending on the MAS frequency and the rotor diameter. To avoid line broadening due to recoupling conditions [9,10] the rf-field amplitude needs to be at least three times the spinning frequency. These high-power conditions limit the applicability for sensitive samples and for long decoupling times.

In this paper, we report progress in "low-power decoupling" where the rf-field strength is lower than the MAS frequency, typically 10–20 kHz. Low-power decoupling significantly reduces the sample heating due to rf irradiation and can be applied for longer time periods. Again, there is a rule of thumb that the rf-field amplitude should be different, by at least a factor of three from the MAS frequency to avoid recoupling [11]. We have shown in an earlier publication [12] that low-power cw decoupling becomes feasible for MAS frequencies faster than 40 kHz in organic or biological solids without significant molecular motion. For compounds with reduced dipolar couplings due to motion this regime starts already at lower MAS frequencies. In addition to a loss in signal height, compared to high-power decoupling, a strong

* Corresponding author. Fax: +41-1-632-1621.
E-mail address: maer@nmr.phys.chem.ethz.ch (M. Ernst).

1090-7807/$ - see front matter © 2003 Elsevier Science (USA). All rights reserved.
doi:10.1016/S1090-7807(03)00155-1

sensitivity to ^{1}H resonance offsets is encountered in cw low-power decoupling (vide infra). In liquid-state NMR it has been known for many years that resonance offset effects in decoupling can be compensated by using multiple-pulse sequences [13]. In this contribution we evaluate decoupling sequences for their use in low-power decoupling under fast MAS and find significant improvements in decoupling efficiency and broadbandedness if multiple-pulse decoupling (XiX) is applied.

Fig. 1 shows three one-dimensional ^{13}C spectra of the fully ^{13}C/^{15}N-labeled dipeptide L-Val-L-Phe recorded under different ^{1}H decoupling conditions at a ^{13}C resonance frequency of 125 MHz and spinning at 50 kHz MAS. In Fig. 1a high-power XiX decoupling using a field strength of $\nu_1 \approx 220$ kHz and an optimized pulse length of $\tau_p = 57\,\mu s$ ($\tau_p/\tau_r = 2.85$ [8]) was used. This spectrum demonstrates the best decoupling we could achieve on this sample. The remaining linewidth is dominated by heterogeneous broadening and non-resolved *J*-couplings. Fig. 1b shows our best multiple-pulse low-power decoupling (vide infra) spectrum of this sample using an rf-field strength of $\nu_1 \approx 13$ kHz ($\tau_p = 76\,\mu s$), corresponding to a reduction in the rf power by a factor 290 compared to high-power decoupling. Fig. 1c was recorded using low-power cw decoupling with an rf-field strength of also $\nu_1 \approx 13$ kHz. A comparison of the three spectra shows that a substantial degradation in decoupling efficiency is observed only for the CH_2 group (Fβ) by going from the high-power to the low-power decoupling regime when using the XiX decoupling sequence. The CH_3 and the quarternary carbons show almost no decrease in line height, while the CH groups show a small decrease. The low-power cw-decoupled spectrum, however, shows reduced line heights for all the protonated carbon resonances.

Fig. 2 shows contour plots of two-dimensional ^{13}C correlation spectra of the same dipeptide. The spectra were recorded at an MAS frequency of 50 kHz using proton-driven spin diffusion as a correlation mechanism with a mixing time of $\tau_m = 500$ ms. The spectrum in Fig. 2a was measured using high-power XiX decoupling with an rf-field amplitude of $\nu_1 \approx 220$ kHz ($\tau_p = 57\,\mu s$) while the spectrum in Fig. 2b was recorded using low-power multiple-pulse decoupling with an rf-field amplitude of $\nu_1 \approx 13$ kHz ($\tau_p = 76\,\mu s$). Except for diagonal and cross-peaks involving CH_2 groups, the two spectra show very similar resolution.

Fig. 3 shows a comparison of the decoupling efficiency of high-power XiX decoupling with $\nu_1 \approx 150$ kHz (Fig. 3a) and low-power XiX decoupling with $\nu_1 \approx 13$ kHz (Fig. 3b) on a sample of saccharose (with natural isotopic abundance) which has considerably narrower lines (FWHH between 14 and 18 Hz). In the low-power proton-decoupled ^{13}C spectrum (Fig. 3b) we observe a significant drop in line intensity for the CH_2 groups (38–46% of the high-power decoupled spectrum) which is accompanied by an increase in linewidth to 37–50 Hz. The CH groups show an increase in linewidth to 20–25 Hz while the line intensity drops to 65–75% of the high-power decoupled spectrum. The quarternary carbon resonance shows the same linewidth and the same intensity as in high-power XiX decoupling. This illustrates that the contribution to the residual line is increased by about 5–10 Hz for CH groups and by about 20–30 Hz for CH_2 groups by going from high-power XiX decoupling to low-power XiX decoupling. The reduction in line intensity depends on the achievable linewidth and, therefore, on the other contributions to the linewidth like the inhomogeneous distribution of

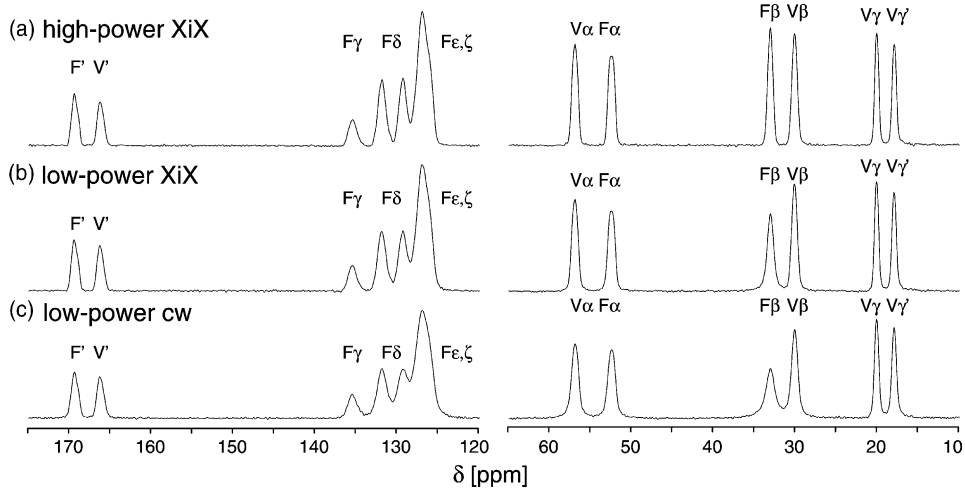

Fig. 1. One-dimensional ^{13}C spectra of the uniformly ^{13}C/^{15}N-labeled dipeptide L-Val-L-Phe measured at an MAS frequency of 50 kHz and for different decoupling conditions: (a) using high-power XiX decoupling with an rf-field amplitude of $\nu_1 \approx 220$ kHz ($\tau_p = 57\,\mu s$); (b) using low-power $(XiX)_{45}$ decoupling with an rf-field amplitude of $\nu_1 \approx 13$ kHz ($\tau_p = 76\,\mu s$); (c) using low-power cw decoupling also with an rf-field amplitude of $\nu_1 \approx 13$ kHz.

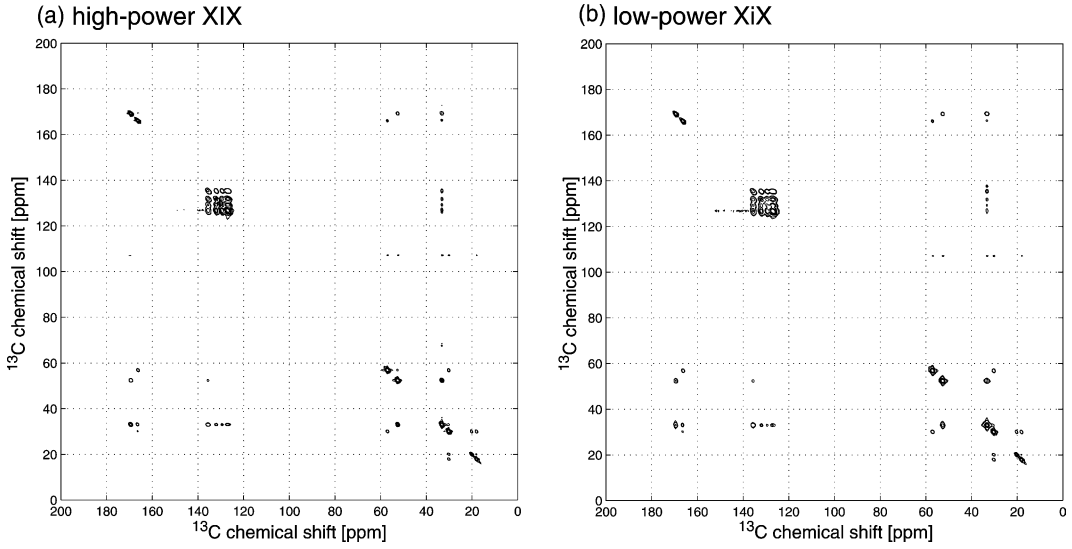

Fig. 2. Two-dimensional ^{13}C chemical-shift correlation spectra of the uniformly ^{13}C/^{15}N-labeled dipeptide L-Val-L-Phe measured at an MAS frequency of 50 kHz using proton-driven spin diffusion as a transfer mechanism. The spectrum in (a) was measured using high-power XiX decoupling with an rf-field amplitude of $\nu_1 \approx 220$ kHz ($\tau_p = 57$ μs) while the spectrum in (b) was recorded using low-power $(XiX)_{45}$ decoupling with an rf-field amplitude of $\nu_1 \approx 13$ kHz ($\tau_p = 76$ μs).

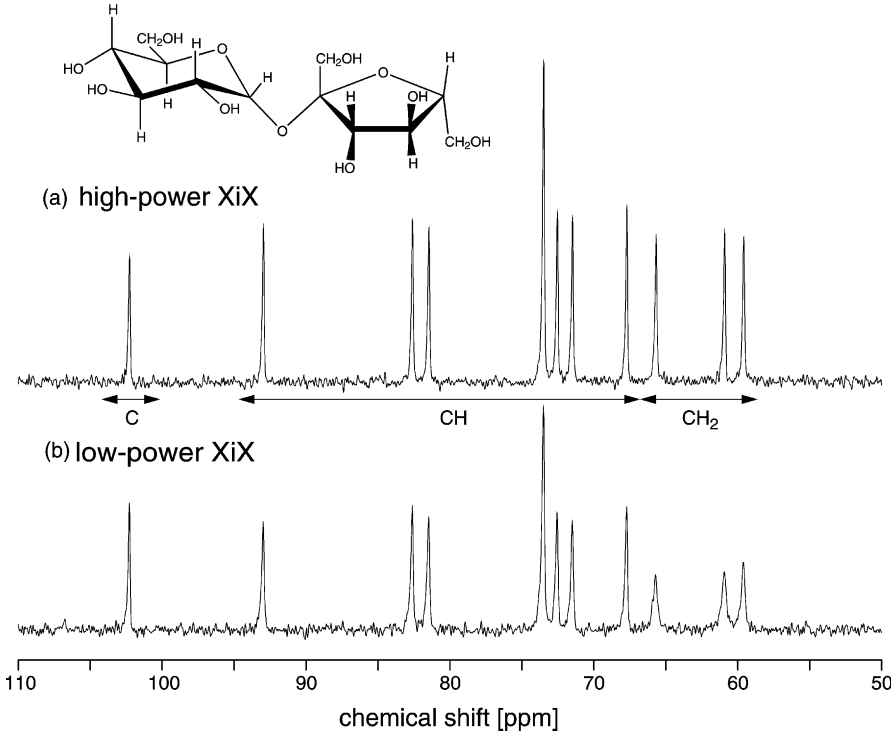

Fig. 3. One-dimensional ^{13}C spectra of saccharose (non-enriched) using (a) high-power XiX decoupling and (b) low-power XiX decoupling. The spinning frequency was 50 kHz and the rf-field strengths were 150 and 13 kHz, respectively.

the isotropic chemical shifts. These two examples clearly illustrate that at spinning frequencies of 50 kHz, low-power multiple-pulse decoupling is an interesting alternative to the traditional high-power decoupling approach.

2. Theory

We consider a model system where a single S spin is coupled to a large number of I spins described by the Hamiltonian:

$$\mathscr{H}(t) = \mathscr{H}_S^{\mathrm{CS}} + \mathscr{H}_I^{\mathrm{CS}} + \mathscr{H}_{II}^{J} + \mathscr{H}_{SI}^{J} + \mathscr{H}_S^{\mathrm{CSA}}(t) + \mathscr{H}_I^{\mathrm{CSA}}(t) + \mathscr{H}_{II}^{\mathrm{dip}}(t) + \mathscr{H}_{SI}^{\mathrm{dip}} + \mathscr{H}_I^{\mathrm{rf}}(t). \quad (1)$$

Here $\mathscr{H}_S^{\mathrm{CS}}$ and $\mathscr{H}_I^{\mathrm{CS}}$ are the isotropic chemical shifts of spins S and I, respectively; $\mathscr{H}_{II}^{\mathrm{I}}$ are the homonuclear and $\mathscr{H}_{SI}^{J}$ the heteronuclear isotropic J-couplings; $\mathscr{H}_S^{\mathrm{CSA}}(t)$ and $\mathscr{H}_I^{\mathrm{CSA}}(t)$ are the time-dependent chemical-shielding contributions from spins S and I, respectively; $\mathscr{H}_{II}^{\mathrm{dip}}(t)$ are the homonuclear and $\mathscr{H}_{SI}^{\mathrm{dip}}(t)$ the heteronuclear time-dependent dipolar couplings; and $\mathscr{H}_I^{\mathrm{rf}}(t)$ is the time-dependent rf irradiation on the I spins. Explicit expressions for the various terms can be found in the literature [14–16].

2.1. Low-power CW decoupling

For applying average Hamiltonian theory to low-power CW decoupling we have to make the simplifying assumption that the rf amplitude ω_1 and the MAS frequency are commensurate, i.e., $q\omega_{\mathrm{r}} = p\omega_1$. Under this condition we can go into an interaction-frame representation with the rf Hamiltonian and use average Hamiltonian theory to obtain a time-independent system Hamiltonian. It is, however, important to keep in mind that depending on the values of p and q the cycle time of the average Hamiltonian can become quite long and the question of the convergence of the average Hamiltonian series is only warranted if p and q have a small common multiple.

If we avoid the HORROR recoupling condition $p/q = 2$ [11], the zeroth-order average Hamiltonian is given by

$$\overline{\mathscr{H}}^{(0)} = \mathscr{H}_S^{\mathrm{CS}} + \mathscr{H}_{II}^{J}. \quad (2)$$

This Hamiltonian describes perfect heteronuclear decoupling independent of the rf amplitude (within the limits defined above). For finite spinning frequencies we have to consider higher orders of the average Hamiltonian. The first-order average Hamiltonian is given by

$$\overline{\mathscr{H}}^{(1)} = \sum_k \left[\frac{p\omega_k^{\mathrm{iso}}\pi J_{Sk}}{\omega_{\mathrm{r}} q} + \frac{pq^3 - p^3 q}{q^4 - 5p^2q^2 + 4p^4} \frac{\omega_{Sk}^{+1}\omega_k^{-1} + \omega_{Sk}^{-1}\omega_k^{+1}}{\omega_{\mathrm{r}}} + \frac{pq^3 - 4p^3 q}{q^4 - 5p^2q^2 + 4p^4} \frac{\omega_{Sk}^{+2}\omega_k^{-2} + \omega_{Sk}^{-2}\omega_k^{+2}}{\omega_{\mathrm{r}}} \right] 2S_z I_{kx}, \quad (3)$$

where only terms involving S-spin operators are shown. Here ω_{Sk}^{m} and ω_k^{m} are the Fourier coefficients of the time-dependent heteronuclear dipolar coupling and the chemical-shielding tensors of the I spins, respectively. Assuming that the rf field is much smaller than the MAS frequency, i.e., for large values of p/q, we can simplify the expression and obtain

$$\overline{\mathscr{H}}^{(1)} \approx \sum_k \left[\frac{p\omega_k^{\mathrm{iso}}\pi J_{Sk}}{\omega_{\mathrm{r}} q} - \sum_{\substack{m=-2 \\ m\neq 0}}^{2} \frac{q\omega_{Sk}^{+m}\omega_k^{-m}}{m^2 p\omega_{\mathrm{r}}} \right] 2S_z I_{kx}. \quad (4)$$

The first term in Eq. (4) is the isotropic off-resonance decoupling cross-term between the heteronuclear J coupling and the chemical-shift offset which is well known [13]. The second term is a cross-term between the chemical-shielding tensor of the I spins and the heteronuclear dipolar-coupling tensor. The $1/\omega_{\mathrm{r}}$ dependence of the dominating residual coupling term in the first-order average Hamiltonian is experimentally manifest in a $1/\omega_{\mathrm{r}}$ dependence of the linewidth for spinning frequencies exceeding 20 kHz (data not shown) [12] where higher-order terms can be neglected. The first-order average Hamiltonian of Eq. (4) has a very similar structure as the leading term in the case of high-power cw decoupling under MAS [17].

2.2. Low-power XiX decoupling

Under a phase-inversion pulse sequence like XiX, the synchronization condition $q\omega_{\mathrm{r}} = p\omega_1$ for calculating an average Hamiltonian is replaced by the condition $q\omega_{\mathrm{r}} = p\omega_{\mathrm{m}}$, i.e., the length of the pulse sequence $2\tau_{\mathrm{p}} = 2\pi/\omega_{\mathrm{m}}$ and the rotor cycle $\tau_{\mathrm{r}} = 2\pi/\omega_{\mathrm{r}}$ must be commensurate while the amplitude of the rf field ω_1 can be arbitrary. We distinguish two situations.

(i) If the pulse length is a multiple of a quarter rotor period, $\tau_{\mathrm{p}} = n\tau_{\mathrm{r}}/4$, the zeroth-order average Hamiltonian contains recoupled dipolar-coupling terms. These unwanted terms vanish only for particular settings of the rf amplitude and pulse length, e.g., for $\tau_{\mathrm{p}}\omega_1 = k2\pi$ and $\tau_{\mathrm{p}} = n\tau_{\mathrm{r}}$. Because decoupling sequences are expected to be tolerant to rf inhomogeneities, we disqualify all sequences with $\tau_{\mathrm{p}} = n\tau_{\mathrm{r}}/4$. This result of the zeroth-order average Hamiltonian is in agreement with the observation that the XiX sequence corresponds to a so-called $C2_n^0$ recoupling sequence [6,18,19] if the pulse length is an integer multiple of a quarter rotor cycle [8].

(ii) If $\tau_{\mathrm{p}} \neq n\tau_{\mathrm{r}}/4$, but still $q\omega_{\mathrm{r}} = p \cdot \omega_{\mathrm{m}}$ with a small common multiple of q and p such that average Hamiltonian theory can successfully be applied, we have found vanishing heteronuclear dipolar contributions to the zeroth-order average Hamiltonian for all the pairs (p, q) that we have calculated ($(p, q) = \{(6n + 2, 3), (6n + 4, 3), (2, 5), (2, 6), (14n + 2, 7), (2, 8), (2, 9), (2, 10)\}$). We have not succeeded in obtaining a general analytical solution for arbitrary values of (p, q). The zeroth-order average Hamiltonian can still contain contributions from the isotropic heteronuclear J-coupling or from the chemical-shift offset of the I spins if the condition $\tau_{\mathrm{p}}\omega_1 = k2\pi$ is not fulfilled. These terms are well-known from decoupling in liquid-state NMR [13] and are, in the present context, less of a concern because of the relatively small values of the J-couplings compared

to the heteronuclear dipolar couplings. If the flip angle of each pulse is a multiple of 2π, we obtain the desired zeroth-order average Hamiltonian

$$\overline{\mathscr{H}}^{(0)} = \mathscr{H}_S^{\mathrm{CS}} + \mathscr{H}_{II}^{J}. \tag{5}$$

Of course, this is not yet an improvement over cw decoupling which also leads to the same zeroth-order average Hamiltonian. We must, therefore, search for conditions that lead also to a vanishing first-order average Hamiltonian. For certain pulse lengths, e.g., for $\tau_p = k\tau_r + \tau_r/3$ and $\tau_p = k\tau_r + 2\tau_r/3$ we find indeed

$$\overline{\mathscr{H}}^{(1)} = 0 \tag{6}$$

if the rf nutation corresponds to an integer multiple of a 2π rotation, i.e., if $\tau_p\omega_1 = k2\pi$. For other rf-field strengths we find that the first-order average Hamiltonian contains terms originating from the product of an isotropic term with an anisotropic term in the Hamiltonian, i.e., cross-terms between the heteronuclear dipolar coupling and the isotropic chemical shift or cross-terms between the heteronuclear isotropic J coupling and the chemical-shielding tensor. We suspect that the findings for our selection of (p, q) are valid for arbitrary pairs as long as we avoid certain multiples of $\tau_p = n\tau_r/6$ and $\tau_p = n\tau_r/8$. Furthermore, we suspect that the cases with two incommensurate time-dependencies behave similar to a close-by commensurate point. We are presently studying these non-synchronous cases in the framework of two-mode floquet theory [20–25].

From our average Hamiltonian calculations we expect that we will obtain best decoupling if the pulse length τ_p is not an integer multiple of a quarter rotor cycle and the flip angle of the pulse is a multiple of a 2π rotation. This will lead to a zeroth-order and first-order average Hamiltonian of zero while deviations in the flip angle due to misadjustment of the rf-field or due to rf-field inhomogeneities will only lead to small terms in the zeroth-order average Hamiltonian originating from the heteronuclear J-couplings. Contributions from the anisotropic dipolar couplings will only appear in the first-order average Hamiltonian. We expect, therefore, a strong dependence of the decoupling quality on the timing of the pulse sequence and also on the precise setting of the flip angle of the pulses. A numerical investigation of the first-order average Hamiltonian terms showed that the magnitude of these terms decreases with an increasing ratio of ω_1/ω_r. This explains the experimental observation that in high-power XiX decoupling the decoupling quality is largely independent of the flip angle [8] (vide infra).

3. Experiments and discussion

All spectra shown here were measured on a Varian Infinity + 500 MHz spectrometer using a a homebuilt 1.8 mm o.d. double-resonance MAS probe capable of spinning up to 50 kHz with a sample volume of about 11 μl [26]. The linewidths obtained in the fully $^{13}C/^{15}N$-labeled dipeptide (L-Val-L-Phe) under high-power XiX decoupling were in the range of 75–120 Hz full width at half height (FWHH). Fig. 4 shows the line height of four

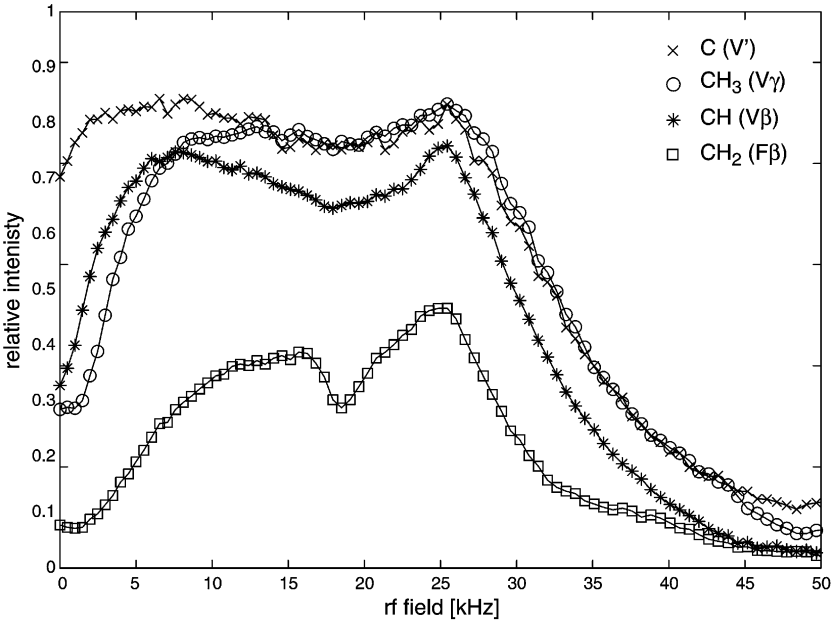

Fig. 4. Line height of four selected carbon resonances in the uniformly $^{13}C/^{15}N$-labeled dipeptide L-Val-L-Phe measured at an MAS frequency of 50 kHz as a function of the decoupler field strength: (×) C' of valine (unprotonated C), (∗) C^{β} of valine (CH group), (□) C^{β} of alanine (CH_2 group), and (◯) C^{γ} of valine (CH_3 group).

selected carbon resonances under cw irradiation in the fully labeled dipeptide as a function of the rf-field amplitude at an MAS frequency of 50 kHz. The line heights were normalized such that the optimized high-power XiX decoupling corresponds to an intensity of one. From Fig. 4 it is obvious that there are two potential regions which could be used to implement multiple-pulse low-power decoupling: (i) rf-field amplitudes from 10 to 15 kHz and rf-field amplitudes around 25 kHz. Experiments showed that for rf-field amplitudes around 25 kHz where cw low-power decoupling performs best, XiX seem to perform significantly worse than cw decoupling while for rf-field amplitudes in the range from 10 to 15 kHz an increase in line height could be observed using XiX.

Fig. 5a shows a contour plot of the line height in [2-^{13}C]-labeled alanine under XiX decoupling as a function of the rf-field amplitude and pulse length. The MAS frequency was set to 50 kHz. One can clearly see that the line intensity is very low, corresponding to bad decoupling, if the pulse length τ_p is a multiple of half the rotor period $\tau_r/2$. In between these strong minima, however, there are plateaus with high line intensities along the line $\nu_1 = 1/\tau_p$, i.e., for pulse lengths corresponding to 2π rotations. There are also weaker maxima along the line $\nu_1 = 2/\tau_p$, i.e., for pulse lengths corresponding to 4π rotations and further optima corresponding to 6π rotations. The maximum line intensity at $\tau_p = 77\,\mu s$ and $\nu_1 \approx 13$ kHz is 75% of the line intensity obtained using high-power XiX decoupling at an rf-field amplitude of 220 kHz. From these measurements, it can clearly be seen that XiX yields good decoupling with low rf fields. However, the decoupling efficiency depends considerably on the rf amplitude, in contrast to high-power XiX decoupling (Fig. 5b).

The decoupling quality of low-power XiX can further be improved by adding a z rotation by an angle ϕ on the basic XiX pulse cycle. This leads to a sequence where the basic $((\tau_p)_{0°}, (\tau_p)_{180°})$ building block is repeated with all phases incremented by an angle ϕ. We call such a decoupling sequence $(XiX)_\phi$. Experimental optimization (data not shown) showed that for a phase shift of $\phi \approx 45°$ the best results were obtained. The increase in signal intensity was in the order of 5% compared to low-power XiX decoupling without a z rotation. In addition, such a sequence showed somewhat better offset compensation (vide infra). The dependence of the decoupling quality (line height) as a function of the pulse length is shown in Fig. 6 for four selected carbon resonances in the fully ^{13}C/^{15}N-labeled dipeptide L-Val-L-Phe using an rf-field strength of $\nu_1 \approx 13$ kHz and an MAS frequency of $\nu_r = 50$ kHz. Again, the line heights are normalized such that the optimized high-power XiX decoupling corresponds to an intensity of one. Best decoupling is achieved around a pulse length of $\tau_p = 76\,\mu s$ for all four types of carbon resonances. For the CH_2 group the efficiency is around 65% compared to high-power XiX decoupling while for all other resonances the line height is larger than 90% compared to high-power XiX decoupling. There are sharp performance minima if the condition $2\tau_p/\tau_r = n$ is fulfilled where n is an integer. Similar resonance conditions have been observed in high-power XiX decoupling [8].

Using low-power XiX decoupling in rotating solids does not only improve the decoupling quality compared to cw decoupling but also reduces the sensitivity to offset

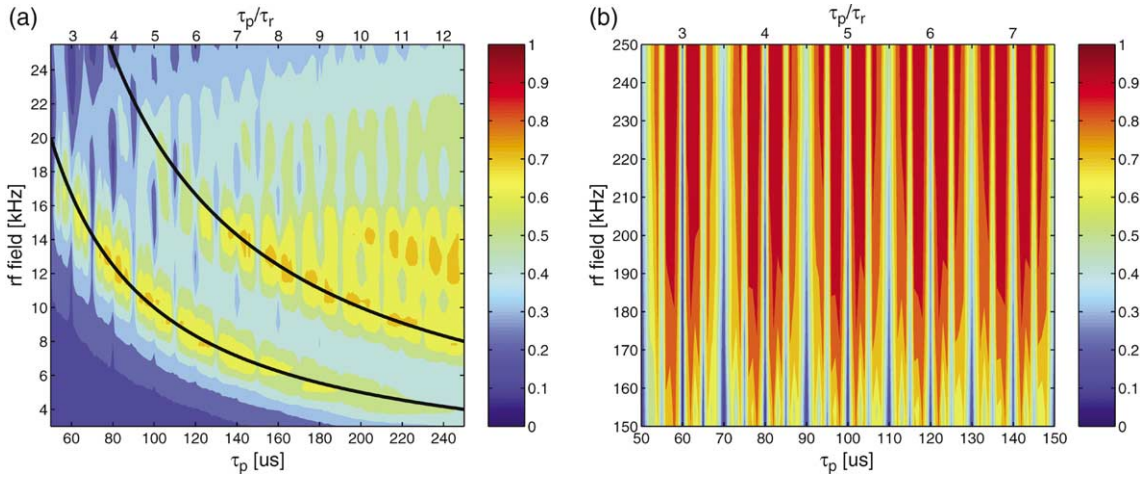

Fig. 5. Contour plots of the line height in [2-^{13}C]alanine as a function of the pulse length (τ_p) and the decoupler field strength (ν_1) at an MAS frequency of 50 kHz for (a) low-power XiX decoupling and (b) high-power XiX decoupling. The thick black lines in (a) show the curves $\nu_1 = 1/\tau_p$ and $\nu_1 = 2/\tau_p$ corresponding to a flip angle of the pulses of 2π and 4π, respectively. One can clearly see that the maxima of the line height appear along these two curves indicating that the flip angle of the pulses should be a multiple of 2π in order to obtain good decoupling. For high-power XiX decoupling (b) no such dependence on the flip angle can be observed. An intensity of one corresponds to the intensity obtained under optimized high-power XiX decoupling.

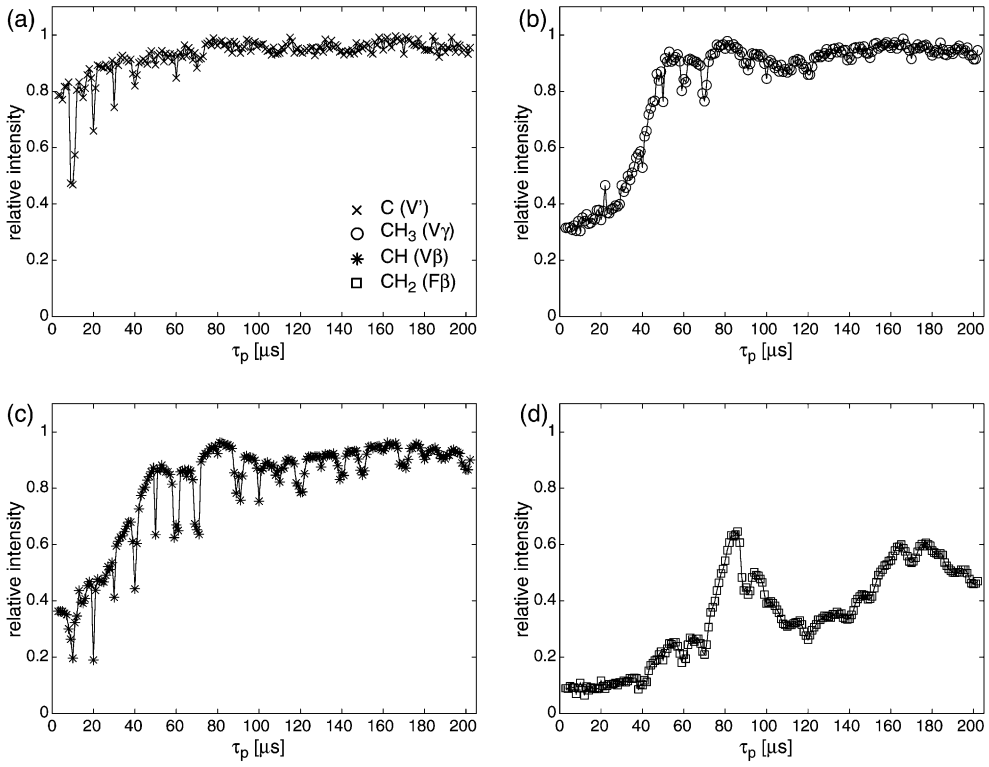

Fig. 6. Line height of four selected carbon resonances in the uniformly $^{13}C/^{15}N$-labeled dipeptide L-Val-L-Phe measured at an MAS frequency of 50 kHz and at an rf-field amplitude $\nu_1 \approx 13$ kHz as a function of the pulse length τ_p: (a) (×) C′ of valine (unprotonated C), (b) (∗) C^β of valine (CH group), (c) (□) C^β of alanine (CH_2 group), and (d) (◯) C^γ of valine (CH_3 group).

effects as predicted by the first-order average Hamiltonians of Eqs. (4) and (6). Fig. 7 shows the experimental ^{1}H-offset dependence of low-power cw decoupling ($\nu \approx 13$ kHz, Fig. 7a) and low-power $(XiX)_{45}$ decoupling ($\nu_1 \approx 13$ kHz, $\tau_p = 76\,\mu s$, Fig. 7b) over a range of 10 kHz corresponding to 20 ppm at 500 MHz proton resonance frequency. The offset dependence for high-power XiX is very weak (data not shown) as one would expect from the large ration of rf-field strength to chemical-shift offsets for protons (±5 kHz). The sensitivity of low-power $(XiX)_{45}$ decoupling to proton chemical-shift offsets is significantly reduced compared to low-power cw decoupling (see Fig. 7a). For the CH_2 group we find a reduction of the intensity by less than 20% in a range of 5 kHz corresponding to 10 ppm at 500 MHz proton resonance frequency. For the other carbon resonances

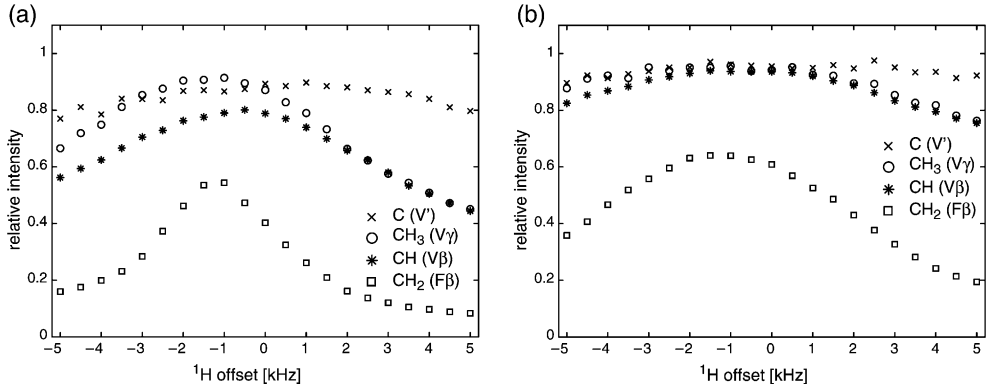

Fig. 7. Line height measured as a function of the ^{1}H carrier frequency for (a) low-power cw decoupling and (b) low-power $(XiX)_{45}$ decoupling at an MAS frequency of 50 kHz. The graphs show the line heights of four selected resonances in a sample of U-^{13}C-^{15}N-L-Val-L-Phe: (×) C′ of valine (unprotonated C), (∗) C^β of valine (CH group), (□) C^β of alanine (CH_2 group), and (◯) C^γ of valine (CH_3 group). The rf-field strength was set to $\nu_1 \approx 220$ kHz ($\tau_p = 57\,\mu s$) and 13 kHz ($\tau_p = 76\,\mu s$), respectively. The line heights were normalized such that optimized high-power XiX decoupling corresponds to one.

we find a reduction of less than 10% over a range of 8 kHz. Both chemical-shift ranges are sufficient to cover the range of typical proton resonance frequencies in organic solids.

4. Conclusions

We have shown that for MAS frequencies of 50 kHz low-power decoupling using the XiX sequences becomes a viable alternative to conventional high-power irradiation using XiX or TPPM decoupling schemes. Only for CH_2 groups a significant line broadening must be tolerated. At 50 kHz MAS frequency the loss in line height we found in a dipeptide was less than 10% for all types of carbon resonances except for CH_2 groups where a decrease in line height by about 40% was found. The amount of loss in line height depends on the sample and the other contributions to the linewidth.

Low-power $(XiX)_{45}$ decoupling seems to work best with an rf-field amplitude corresponding to a nutation frequency of about 1/4 of the MAS frequency. High-power decoupling usually requires the rf-field amplitude to be at least three times the MAS frequency to avoid rotary-resonance conditions [9,10]. Therefore, we can expect a reduction in rf-field amplitude by at least a factor of 12. This reduction in rf power is especially important for temperature-sensitive samples like biological macromolecules. One can also imagine that low-power decoupling might be of advantage to be used during the mixing time in a two-dimensional correlation experiment.

It is reasonable to expect that low-power decoupling will further improve with increasing MAS frequencies due to a better averaging of the higher-order average Hamiltonian terms that contain anisotropic spin interactions as well as chemical-shift offsets. A better understanding of the theoretical background of multiple-pulse decoupling may also lead to improved low-power decoupling sequences for rotating solids.

Acknowledgments

We thank the "Swiss Baltic Net" of the Gerbert Rüf Stiftung for supporting the collaboration between Tallinn and Zürich. Financial support by the Swiss National Science Foundation and the Estonian Science Foundation is gratefully acknowledged.

References

[1] A.E. Bennett, C.M. Rienstra, M. Auger, K.V. Lakshmi, R.G. Griffin, J. Chem. Phys. 103 (1995) 6951–6958.
[2] Z.H. Gan, R.R. Ernst, Solid State NMR 8 (1997) 153–159.
[3] Y. Yu, B.M. Fung, J. Magn. Reson. 130 (1998) 317–320.
[4] B.M. Fung, A.K. Khitrin, K. Ermolaev, J. Magn. Reson. 142 (2000) 97–101.
[5] K. Takegoshi, J. Mizokami, T. Terao, Chem. Phys. Lett. 341 (2001) 540–544.
[6] M. Eden, M.H. Levitt, J. Chem. Phys. 111 (1999) 1511–1519.
[7] P. Tekely, P. Palmas, D. Canet, J. Magn. Reson. A 107 (1994) 129–133.
[8] A. Detken, E.H. Hardy, M. Ernst, B.H. Meier, Chem. Phys. Lett. 356 (2002) 298–304.
[9] T.G. Oas, R.G. Griffin, M.H. Levitt, J. Chem. Phys. 89 (1988) 692.
[10] M.H. Levitt, T.G. Oas, R.G. Griffin, Isr. J. Chem. 28 (1988) 271–282.
[11] N.C. Nielsen, H. Bildsoe, H.J. Jakobsen, M.H. Levitt, J. Chem. Phys. 101 (1994) 1805.
[12] M. Ernst, A. Samoson, B.H. Meier, Chem. Phys. Lett. 348 (2001) 293–302.
[13] R.R. Ernst, G. Bodenhausen, A. Wokaun, Principles of Nuclear Magnetic Resonance in One and Two Dimensions, Clarendon Press, Oxford, 1987.
[14] M. Mehring, Principles of High Resolution NMR in Solids, second ed., Springer, Berlin, 1983.
[15] U. Haeberlen, High Resolution NMR in Solids: Selective Averaging, Academic Press, New York, 1976.
[16] K. Schmidt-Rohr, H.W. Spiess, Multidimensional Solid-State NMR and Polymers, Academic Press, London, 1994.
[17] M. Ernst, S. Bush, A.C. Kolbert, A. Pines, J. Chem. Phys. 105 (1996) 3387–3397.
[18] Y.K. Lee, N.D. Kurur, M. Helmle, O.G. Johannessen, N.C. Nielsen, M.H. Levitt, Chem. Phys. Lett. 242 (1995) 304.
[19] A. Brinkmann, M.H. Levitt, J. Chem. Phys. 115 (2001) 357–384.
[20] T.S. Ho, S.-I. Chu, J.V. Tietz, Chem. Phys. Lett. 96 (1983) 464.
[21] T.S. Ho, S.-I. Chu, J. Phys. B 17 (1984) 2101.
[22] T.S. Ho, S.-I. Chu, Phys. Rev. A 31 (1985) 659.
[23] M. Baldus, T.O. Levante, B.H. Meier, Z. Naturforsch. A 49 (1994) 80–88.
[24] T.O. Levante, M. Baldus, B.H. Meier, R.R. Ernst, Mol. Phys. 86 (1995) 1195–1212.
[25] E. Vinogradov, P.K. Madhu, S. Vega, J. Chem. Phys. 115 (2001) 8983–9000.
[26] A. Samoson, T. Tuherm, J. Past, J. Magn. Reson. 149 (2001) 264–267.